This article is a *Plant Cell* Advance Online Publication. The date of its first appearance online is the official date of publication. The article has been edited and the authors have corrected proofs, but minor changes could be made before the final version is published. Posting this version online reduces the time to publication by several weeks.

Maize RNA Polymerase IV Defines *trans*-Generational Epigenetic Variation[W]

Karl F. Erhard, Jr.,[a,1] Susan E. Parkinson,[a] Stephen M. Gross,[a,2,3] Joy-El R. Barbour,[b,4] Jana P. Lim,[a,5] and Jay B. Hollick[a,4,6]

[a] Department of Plant and Microbial Biology, University of California, Berkeley, California 94720-3102
[b] Department of Molecular Cell Biology, University of California, Berkeley, California 94720-3200

The maize (*Zea mays*) RNA Polymerase IV (Pol IV) largest subunit, RNA Polymerase D1 (RPD1 or NRPD1), is required for facilitating paramutations, restricting expression patterns of genes required for normal development, and generating small interfering RNA (siRNAs). Despite this expanded role for maize Pol IV relative to *Arabidopsis thaliana*, neither the general characteristics of Pol IV–regulated haplotypes, nor their prevalence, are known. Here, we show that specific haplotypes of the *purple plant1* locus, encoding an anthocyanin pigment regulator, acquire and retain an expanded expression domain following transmission from siRNA biogenesis mutants. This conditioned expression pattern is progressively enhanced over generations in Pol IV mutants and then remains heritable after restoration of Pol IV function. This unusual genetic behavior is associated with promoter-proximal transposon fragments but is independent of sequences required for paramutation. These results indicate that *trans*-generational Pol IV action defines the expression patterns of haplotypes using co-opted transposon-derived sequences as regulatory elements. Our results provide a molecular framework for the concept that induced changes to the heterochromatic component of the genome are coincident with heritable changes in gene regulation. Alterations of this Pol IV–based regulatory system can generate potentially desirable and adaptive traits for selection to act upon.

INTRODUCTION

Epialleles, epigenetic variants of isogenic alleles, are characterized in diverse eukaryotes as non-DNA-based sources of regulatory variation (Jablonka and Raz, 2009). One potential link between many mitotically, and sometimes meiotically, heritable epiallele states is their association with nearby repetitive DNA sequences, such as transposable elements (TEs) (Slotkin and Martienssen, 2007). TE sequences provide host genomes with a rapidly evolving source of gene regulatory capacity, as shown recently in maize (*Zea mays*) where a *Hopscotch* family retrotransposon insertion functions as an enhancer in specific haplotypes of a domestication locus (Studer et al., 2011). Though the prevalence of heritable epialleles in natural populations remains unknown (Richards, 2011), epigenetic regulation of endogenous haplotypes associated with TEs could provide a significant source of adaptive phenotypes that are *trans*-generationally stable, yet reversible under certain conditions.

Specific maize haplotypes that undergo paramutation can be considered *trans*-generationally stable epialleles that are unique in their ability to alter meiotically heritable regulatory states via *trans*-homolog interactions (Erhard and Hollick, 2011). Several maize haplotypes known to participate in paramutation interactions contain *cis*-regulatory elements that are repetitive in nature, and these examples provide experimental models for understanding the mechanism of regulation for repeat-associated epialleles (Erhard and Hollick, 2011). In a species such as maize, where the genome is composed of >85% TEs (Schnable et al., 2009) and haplotype diversity between inbred lines is driven predominantly by TE mobilization (Wang and Dooner, 2006), a large number of TE-associated epialleles is possible.

Paramutation is typified by the distinct regulatory states and inheritance patterns exhibited by *Pl1-Rhoades* haplotypes of the *purple plant1* (*pl1*) locus. When combined in a heterozygote, a *Pl1-Rhoades* haplotype in the strongly expressed *Pl-Rh* state becomes repressed in trans by a homologous haplotype existing in a weakly expressed *Pl′* state and acquires the meiotically heritable *Pl′* state during development (Hollick et al., 1995). The paramutation mechanism remains unknown, though several proteins required for producing 24-nucleotide RNAs, usually termed small interfering RNAs (siRNAs), are required for maintaining repressed *Pl′* states, as well as repressed states of other maize haplotypes subject to paramutation (Erhard and Hollick, 2011). siRNAs present in both maize (Nobuta et al., 2008; Barbour et al., 2012) and *Arabidopsis thaliana* (Kasschau et al., 2007) are highly enriched for sequences of TEs and other repeats. These

[1] Current address: Children's Hospital Oakland Research Institute, Oakland, CA 94609.
[2] Current address: Department of Energy, Joint Genome Institute, Walnut Creek, CA 94598.
[3] Current address: Genomics Division, Lawrence Berkeley National Laboratory, Berkeley, CA 94720.
[4] Current address: Department of Molecular Genetics, The Ohio State University, Columbus, OH 43210.
[5] Current address: Department of Genetics, Stanford University, Stanford, CA 94305.
[6] Address correspondence to hollick.3@osu.edu.
The author responsible for distribution of materials integral to the findings presented in this article in accordance with the policy described in the Instructions for Authors (www.plantcell.org) is: Jay B. Hollick (hollick.3@osu.edu).
[W] Online version contains Web-only data.
www.plantcell.org/cgi/doi/10.1105/tpc.112.107680

observations indicate a link between paramutation-based repression and cellular mechanisms presumably evolved to suppress potential deleterious effects of TE activity.

Plants use specialized RNA polymerases IV and V (Pols IV and V) to facilitate RNA-directed DNA methylation (RdDM) of repetitive genomic sequences via the production and targeting of 24-nucleotide siRNAs. Mutational analyses of genes encoding Pol IV– and V–specific subunits indicate that Pol IV acts upstream in this pathway, generating siRNA precursors, while Pol V acts downstream, generating nascent scaffold transcripts that mediate targeting of siRNAs to homologous loci (Haag and Pikaard, 2011). This siRNA-targeting process guides the deposition of chromatin marks, such as asymmetric (non-CG) cytosine methylation (Haag and Pikaard, 2011), presumably via recruitment of enzymes, such as de novo cytosine methyltransferases.

The biological importance of Pol IV/V-dependent chromatin modifications in *Arabidopsis* has remained unclear, as Pol IV/V subunits are largely dispensable for development, though Pol IV mutant plants are slightly delayed in flowering (Haag and Pikaard, 2011). In maize, the Pol IV largest subunit, RNA Polymerase D1 (RPD1 or NRPD1), is required for facilitating paramutations (Erhard et al., 2009) and for restricting the expression patterns of certain genes required for normal development (Parkinson et al., 2007). These results indicate an expanded role for Pol IV in maize, which is likely related to the higher TE load (Schnable et al., 2009) and more frequent juxtaposition of TEs and genes in the maize genome compared with *Arabidopsis* (Hale et al., 2009). *Pl1-Rhoades* and its derivatives are useful models for studying Pol IV function because their expression states and inheritance patterns can be visually tracked by pigmentation that is most apparent in the anthers of male flowers (Hollick et al., 2000). Here, we show that Pol IV defines the tissue-specific regulation of certain *pl1* alleles through its *trans*-generational action on attendant DNA transposon fragments.

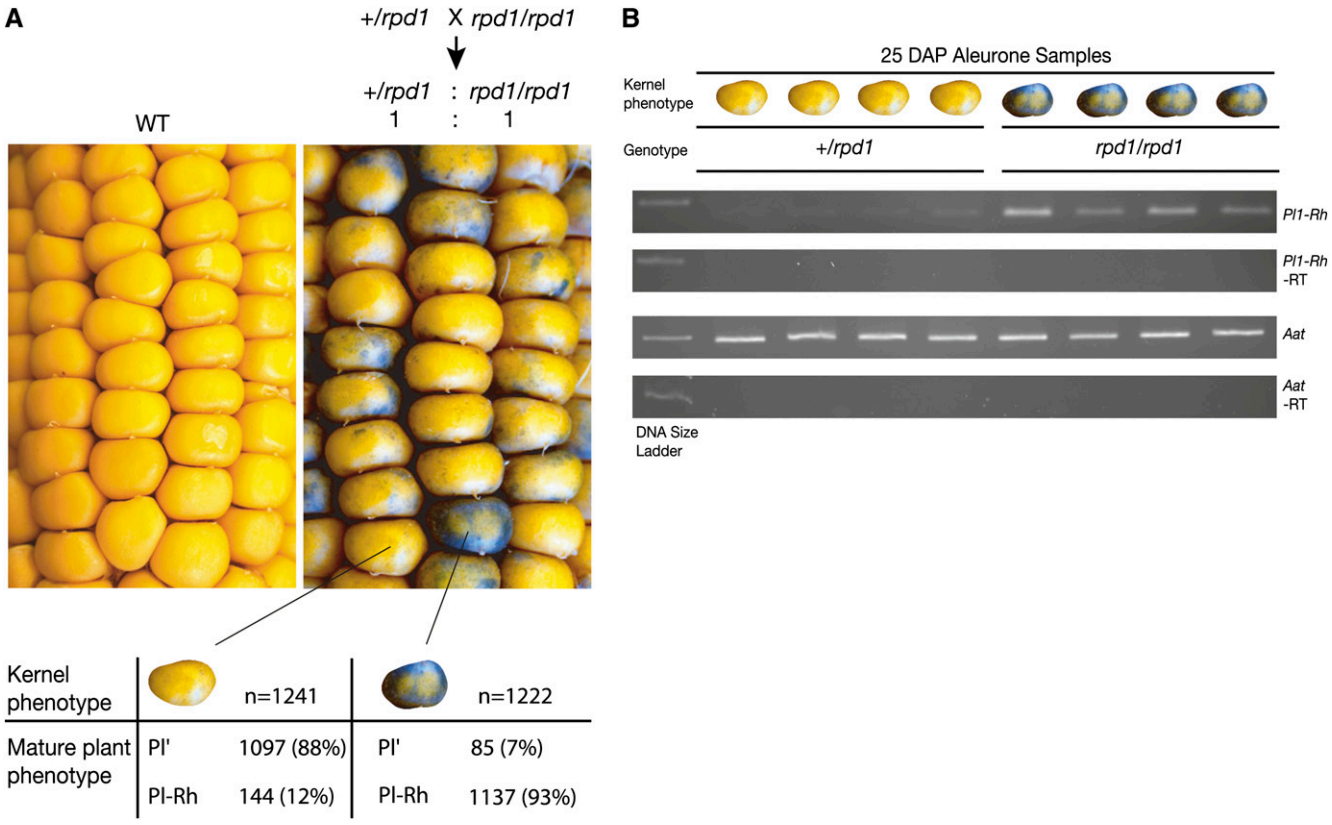

Figure 1. RPD1 Function Represses *Pl1-Rhoades* Expression in the Aleurone.

(A) Aleurone pigment phenotypes in representative wild-type (WT) ears on the left and in ears segregating 1:1 for +/*rpd1* heterozygotes and *rpd1*/*rpd1* homozygotes on the right. Table below shows correlations of anther pigmentation phenotypes (scored at the time of flowering) among ear progeny described above after selection of kernels with the lightest and darkest pigmentation phenotypes, respectively. Pl′(+/*rpd1* genotypes) signifies weak anther pigmentation and Pl-Rh (*rpd1*/*rpd1* genotypes) strong anther pigmentation.

(B) RT-PCR analysis of RNAs isolated from individual aleurones of lightly pigmented (n = 4) and darkly pigmented developing kernels (n = 4) 25 days after pollination (DAP). Below kernel phenotypes are results of molecular genotyping for each individual (see Methods). Primers specific to the *Pl1-Rhoades* (*Pl1-Rh*) allele and a control gene *Ala aminotransferase* (*Aat*) (see Methods) were used to amplify identical quantities of oligo(dT)-primed cDNA templates; amplifications using control samples prepared with no reverse transcriptase (-RT) are shown below for each primer pair.

RESULTS

Absence of RNA Pol IV Reverts a Null Pigment Phenotype

Anthocyanin pigmentation in maize requires function from either the *pl1* locus or its subfunctionalized paralog *colored1* (*c1*) (Cone et al., 1993a): *c1* alleles condition pigmentation of the aleurone, the outermost layer of the kernel endosperm, whereas most *pl1* alleles condition pigmentation of only the vegetative and floral tissues of the plant (Cone et al., 1993a).

Unexpectedly, we observed various degrees of aleurone pigmentation (Figure 1) in progeny segregating 1:1 for *rpd1* homozygous mutants and *+/rpd1* heterozygotes in a background genetically null (*c1/c1*; *Pl1-Rhoades/Pl1-Rhoades*) for aleurone pigmentation (Figure 1A, left panel). Sequencing of the *c1* allele resident in our *rpd1* mutant stocks (see Methods) identified a 363-bp miniature inverted-repeat transposable element of the *Heartbreaker* (*Hbr*) family (Zhang et al., 2000) (see Supplemental Figure 1 online) in exon 2, which introduces a premature nonsense codon that likely renders this *c1-Hbr* allele nonfunctional. We also observed aleurone pigmentation in individuals homozygous for *c1-n* (see Supplemental Table 1 online), a null *c1* allele disrupted by several indels in its coding region (Scheffler et al., 1994). It was therefore unlikely that the aleurone pigmentation seen in the 1:1 segregating *rpd1* lines described above is due to C1. These results indicate that Pol IV is responsible for the colorless kernel phenotype seen in many of our *Pl1-Rhoades* stocks.

Pol IV Restricts Tissue-Specific Expression of *Pl1-Rhoades*

Aleurone and anther pigmentation phenotypes documented over nine generations of 1:1 segregating *rpd1* progeny showed that 93% of the darkest kernel classes correlated with Pl-Rh–like types (both *rpd1-1/rpd1-1* and *rpd1-2/rpd1-2* genotypes) and 88% of the lightest-colored and colorless kernel classes correlated with Pl′-like types (both *+/rpd1-1* and *+/rpd1-2* genotypes) (Figure 1A). Because of this strong correlation, we hypothesized that expansion of *Pl1-Rhoades* expression to the aleurone caused the observed kernel pigmentation seen in the absence of Pol IV. RT-PCR analysis (Figure 1B) of RNAs isolated from four darkly pigmented and four colorless aleurones indicated that *Pl1-Rhoades* RNA levels qualitatively correlated with the amount of aleurone pigmentation for these eight samples. Molecular genotyping for the *rpd1-1* lesion (see Methods) confirmed that the aleurone phenotype reflected the presence (colorless) or absence (darkly pigmented) of RPD1 function (Figure 1B). These results indicate the aleurone pigmentation seen in our stocks results from an expansion of *Pl1-Rhoades* expression, conditioned by passage through *rpd1* mutants.

Trans-Generational Absence of Pol IV Conditions a Fully Colored Kernel Phenotype

The intensity of aleurone pigmentation increased over generations in which *Pl1-Rhoades* was maintained in an *rpd1* mutant background. We generated progeny ears representing different filial generations of 1:1 segregating *rpd1-1* families (Figure 2A) during the same field season to control for environmental conditions and observed a progressive enhancement of *Pl1-Rhoades* expression in the aleurone over an increasing number of generations without RPD1 function. Quantification of five roughly graded classes of aleurone pigmentation (see Supplemental Figure 2A online) in the sibling cross progeny described (Figure 2A) confirmed a *trans*-generational increase in overall aleurone pigmentation (Figure 2B). Notably, by the F5 generation, some kernels had a fully colored phenotype (see Supplemental Figures 2A and 2B online) indistinguishable from that conferred by dominant *C1* alleles (see Supplemental Figure 2C online), and the ratio of this *C1*-like class among ear progeny increased across generations (Figure 2B). These data indicate that *Pl1-Rhoades*, which lacks aleurone expression in reference state nonmutant backgrounds, can be

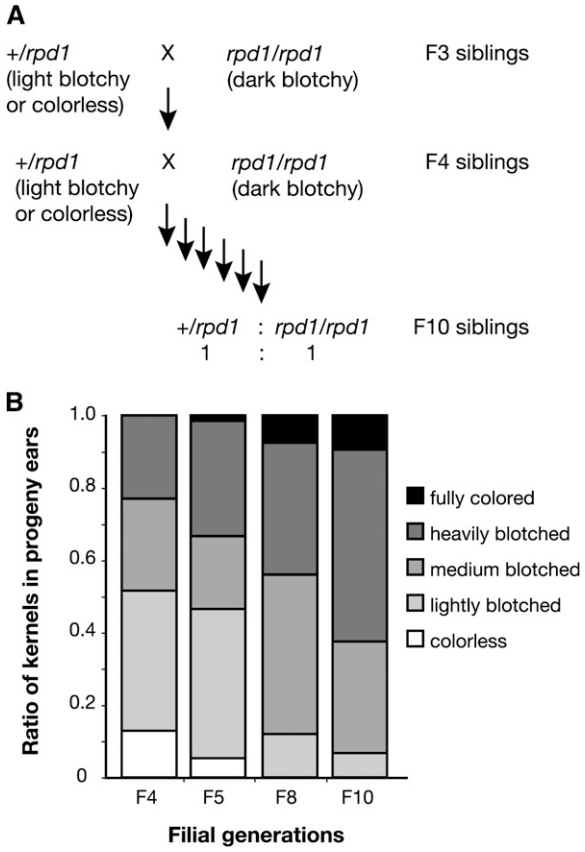

Figure 2. *Trans*-Generational Conditioning of Aleurone Pigmentation in *rpd1* Mutants.

(A) Crossing scheme used to generate inbred lineage of ear progeny that segregate 1:1 for *+/rpd1* heterozygotes and *rpd/rpd1* homozygotes; each arrow signifies a sibling cross, and the details are shown for only two. All crosses were between *+/rpd1* female parents and *rpd1/rpd1* male parents, grown from colorless or lightly blotched kernels and from heavily blotched or fully colored kernels, respectively.

(B) Representative ears were chosen from the lineage described in **(A)** to compare the amount of aleurone pigmentation across generations of progeny. All kernels from ears representing an F4 (n = 279), F5 (n = 189), F8 (n = 241), and F10 (n = 149) filial generation were sorted into the classes of pigmentation (see Supplemental Figure 2A online) listed in the graph and counted. The y axis shows the ratio of the individual kernel class among the total number of kernels for each individual ear.

inherited in a fully functional aleurone expression state after several generations of conditioning in the absence of RPD1 function.

Phenotypes resulting from epigenetic changes are often not heritable across meiosis (Jablonka and Raz, 2009). However, *Pl1-Rhoades* aleurone expression, conditioned in the absence of RPD1 function, was heritable though not 100% penetrant in F1 progeny having inherited at least one copy of wild-type *Rpd1* from either the ear or pollen parent (see Supplemental Table 2 online). This expanded expression domain was also heritable for at least two meiotic cycles in the presence of RPD1 function (see Supplemental Table 2 online).

Conditioned *pl1* Aleurone Expression Is Correlated with a Proximal CACTA-Like Transposon Fragment

Conditioned *Pl1-Rhoades* aleurone expression resembles the expression pattern of *Pl1-Blotched* (Cocciolone and Cone, 1993), a haplotype structurally similar to *Pl1-Rhoades* (Hoekenga et al., 2000) that does not undergo paramutation (Hollick et al., 2000; Gross and Hollick, 2007). We tested the effect of RPD1 loss on the aleurone expression of *Pl1-Blotched* alleles and observed increases from a weak, variegated phenotype (Figure 3A) to fully colored *C1*-like phenotypes among F2S2 progeny of *rpd1-1* mutants (Figure 3B). This result indicates that sequences targeted by Pol IV and regulating aleurone expression are shared between *Pl1-Rhoades* and *Pl1-Blotched* but are insufficient for paramutation. Both alleles contain a 402-bp terminal fragment of a CACTA-like DNA transposon related to the *doppia* subfamily (Cone et al., 1993b) located 97 bp 5′ of the annotated transcription start sites (Figure 3C).

We also observed aleurone pigmentation (see Supplemental Figure 3 and Supplemental Table 3 online) in progeny segregating 1:3 for *rpd1-2* (formerly *rmr6-2*) mutant alleles (Hollick et al., 2005) and a distinct *pl1* variant from the CML52 inbred line, *Pl1-CML52* (Figure 3C), which does not display aleurone expression in nonmutant backgrounds (see Methods). Unlike *Pl1-Blotched*, however, *Pl1-CML52* undergoes paramutation (see Supplemental Table 4 online). Sequencing of the *Pl1-CML52* 5′ region (see

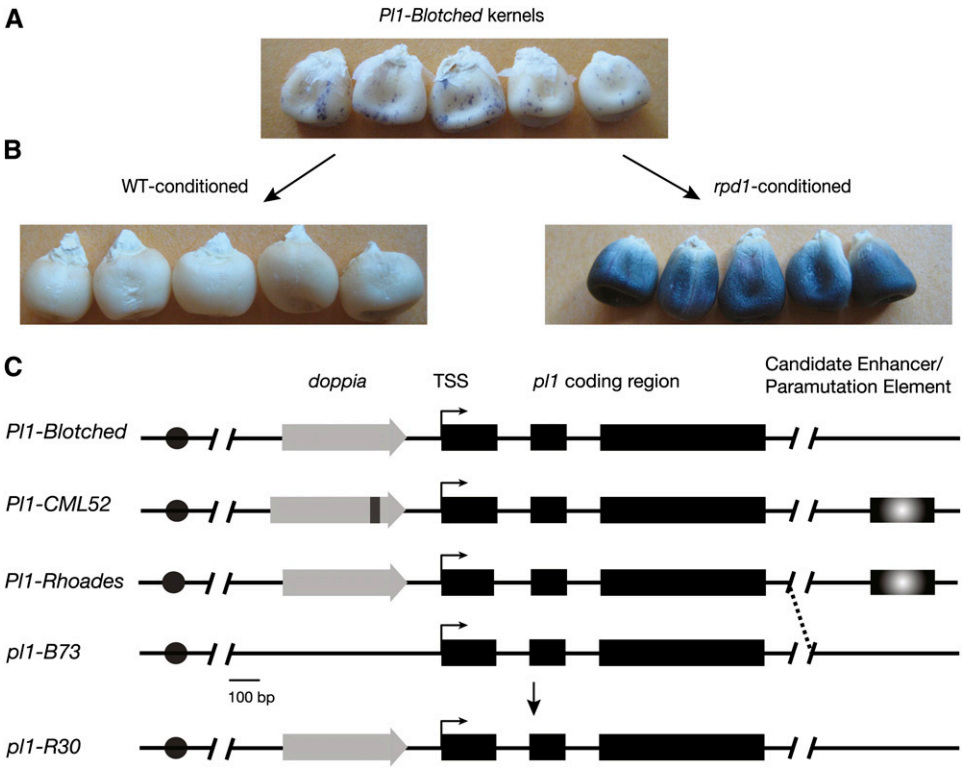

Figure 3. Conditioned *pl1* Aleurone Expression Is Correlated with a Proximal CACTA-Like Transposon Fragment.

(A) Typical *Pl1-Blotched*–conditioned aleurone pigmentation.

(B) Right image shows fully colored, *C1*-like kernels of F2S2 progeny generated by selfing a *Pl1-Blotched*/*Pl1-Blotched*; *rpd1-1*/*rpd1-1* individual. Left image shows F2S2 progeny generated by selfing a *Pl1-Blotched*/*Pl1-Blotched* individual that was either +/+ or +/*rpd1-1*. WT, the wild type.

(C) Diagram of haplotype structures of *pl1* variants used in this study, highlighting the presence of the 5′ *doppia* fragment (gray arrow) and the 3′ candidate enhancer/paramutation region (shaded box). Black circles represent the chromosome 6 centromere, black boxes represent the three exons of the *pl1* coding region, and arrows represent the transcription start site (TSS) of *pl1*. The dark-gray bar in the *Pl1-CML52 doppia* fragment represents a 32-bp indel polymorphism with respect to *Pl1-Rhoades*, *Pl1-Blotched*, and *pl1-R30*. Dotted line between *Pl1-Rhoades* and *pl1-B73* indicates the recombination event that generated *pl1-R30*, a *Pl1-Rhoades* derivative defined genetically by its loss of distal regulatory sequences required for both enhanced expression of and paramutation between *Pl1-Rhoades* alleles (see Methods; see Supplemental Figure 4 online; Figure 4, Tables 1 and 2).

Methods) identified a *doppia* fragment in the same location with respect to the two *pl1* haplotypes described above but containing a 32-bp insertion (Figure 3C). Thus, all three *pl1* haplotypes restricted from aleurone expression via RPD1 action contain a similar proximal DNA transposon fragment.

Sequences Required for Aleurone Expression Are Separable from Those Necessary for Paramutation

Analyses of a *Pl1-Rhoades* derivative, *pl1-R30*, supported the hypothesis that *pl1* aleurone expression is driven by *doppia* sequences found in *pl1* promoter regions. The *pl1-R30* haplotype (Figure 3C) was identified in a screen for recombinant *Pl1-Rhoades* derivatives defective for paramutation (see Methods; see Supplemental Figures 4A and 4B and Supplemental Table 5 online).

We applied sequential selections to identify potential recombinants between *Pl1-Rhoades* and *pl1-B73*, a *pl1* haplotype that does not facilitate paramutation (Gross and Hollick, 2007). Using phenotypic and molecular markers diagnostic of a specific *T6-9* chromosome (*T*) containing *Pl1-Rhoades* in a paramutant *Pl′* state (*T Pl′*), we selected for plants having potentially recombinant chromatids that contained the *Pl1-Rhoades* coding region but lacked ability to facilitate paramutation of *Pl-Rh* in trans (see Supplemental Figure 4B and Supplemental Table 5 online). One individual (06-932-30) had an anther color score (ACS) of 7, the fully colored phenotype expected if paramutation had not occurred (Hollick et al., 1995) (see Supplemental Figure 4C online).

Molecular analyses of genomic DNA from individual 06-932-30 confirmed the presence of a recombinant chromatid having a derivative *pl1* haplotype hereafter referred to as *pl1-R30*. DNA gel blot results (see Supplemental Figure 5 online) showed that *pl1-R30* maintains a *Pl1-Rhoades*–like structure for at least 6 kb 3′ of the coding region, yet PCR results identified *pl1-B73* haplotype polymorphisms at more distal 3′ simple sequence length polymorphism (SSLP) markers *bnlg2249* (~27 Mb away) and *umc2006* (~5 Mb away) (see Supplemental Figures 4C and 4D online). Based on these results and the design of the recombination screen, *pl1-R30* represents a derivative *pl1* haplotype consisting of centromere proximal 5′ sequences, coding region, and 3′ flanking sequences from *Pl1-Rhoades* with more distal 3′ sequences from *pl1-B73*. The exact crossover point remains unknown but is located between ~6 kb and 5 Mb 3′ of the coding region.

Additional genetic tests confirmed that *pl1-R30* was deficient for facilitating paramutation (Table 1; see Supplemental Tables 6 and 7 online). The *pl1-R30* haplotype was combined with *Pl′* and resulting heterozygotes were reciprocally crossed to *Pl-Rh/Pl-Rh* testers. The progeny sets segregated both Pl′-type and Pl-Rh–type plants (Table 1), which was unexpected if *pl1-R30* was able to facilitate paramutation. Because *pl1-R30* was carried on the *T6-9* chromosome, we were able to distinguish most of the *pl1-R30/Pl-Rh* progeny as these had semisterile pollen. All but four of the 29 semisterile plants had fully colored anthers, indicating that paramutation had not occurred (Table 1). The four other semisterile plants had high ACSs that are not typical of paramutant *Pl′*. In total, the *pl1-R30* haplotype is deficient for functions required to acquire and/or facilitate paramutation.

Coincidently, the *pl1-R30* recombinant also lost high levels of expression in seedling sheaths (Figure 4A; see Supplemental Table 8 online), mature leaves (Figure 4B), and anthers as measured by visual assessment of pigment phenotype (Figure 4C; see Supplemental Tables 6 and 8 online) and by RT-PCR (see Supplemental Figure 6 online). These results are consistent with the hypothesis that 3′ sequences required to facilitate paramutation also serve as an enhancer-like element.

We selected pigmented kernels from progeny segregating *pl1-R30*, *Pl1-Rhoades*, and *rpd1-1* alleles, and molecular genotyping (see Methods) confirmed that 6/33 individuals grown from these kernels were homozygous for the *pl1-R30* allele (Table 2). These results show that the 3′ sequences required for paramutation interactions between *Pl1-Rhoades* alleles are not required for *pl1-R30* to be expressed in the aleurone.

Combined, our allelic series comparisons indicate that sequences targeted by Pol IV and regulating aleurone expression are shared between *pl1* haplotypes containing a proximal *doppia* fragment (Figure 3C). Additionally, plants homozygous for *Pl1-Blotched* and *pl1-R30* alleles, which in wild-type backgrounds confer variegated and weak anther pigmentation phenotypes, respectively, also produce dark Pl-Rh–like anther phenotypes in the absence of RPD1 function (see Supplemental Table 9 online). This observation indicates that loss of Pol IV function conditions an overall increase in the expression of *doppia*-associated *pl1* haplotypes, in addition to an apparent expansion of tissue-specific expression in the absence of sequences necessary for paramutation.

Because the *Pl1-Rhoades* promoter-proximal *doppia* is a presumed target of Pol IV–facilitated RdDM (Hale et al., 2007), we asked whether loss of *doppia* cytosine methylation correlated

Table 1. Anther Phenotypes of Progeny Resulting from Reciprocal Crosses of *Pl′/T pl1-R30* and *Pl-Rh/Pl-Rh*

Female Parent	Male Parent	Progeny Structural Genotype	No. of Progeny Sets	No. of Progeny Individuals with Indicated ACS						
				1	2	3	4	5	6	7
Pl-Rh/Pl-Rh	*Pl′ /T pl1-R30*	+/+	2	0	0	7	7	0	0	1
		+/*T*		0	0	0	0	0	1	8
Pl′ /T pl1-R30	*Pl-Rh/Pl-Rh*	+/+	3	1	3	14	5	2	2	0
		+/*T*		0	0	0	0	2	1	17
Totals		+/+	5	1	3	21	12	2	2	1
		+/*T*		0	0	0	0	2	2	25

Pl-Rh/Pl-Rh (A619) was used in all test crosses.

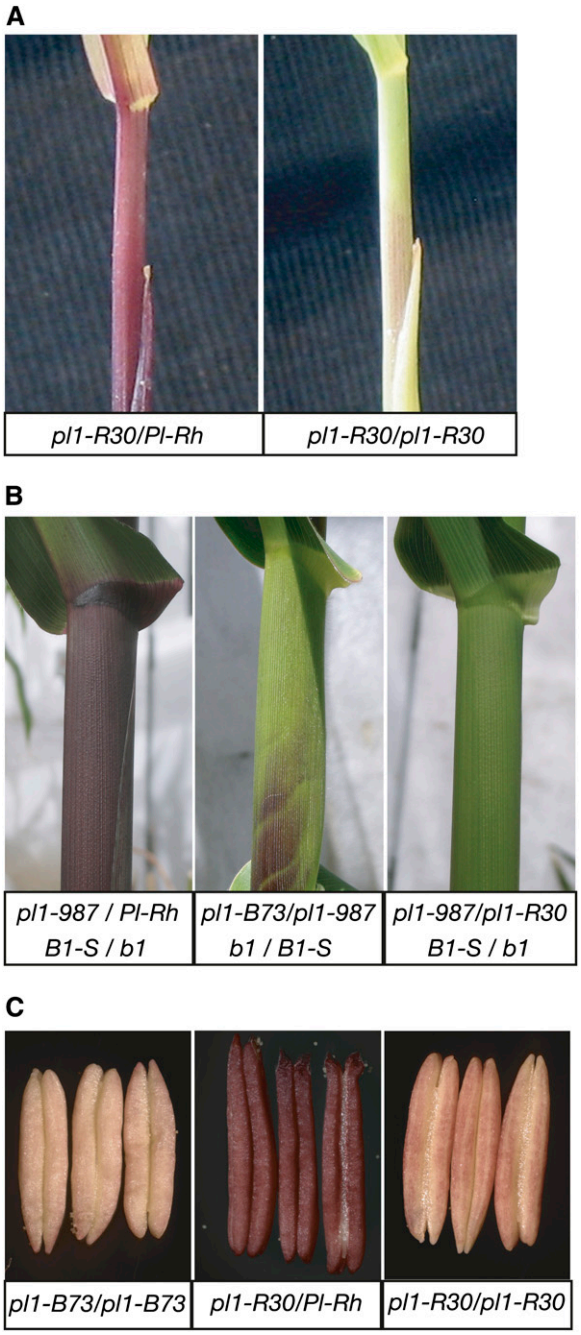

Figure 4. Pigment Phenotypes Conditioned by the *pl1-R30* Allele.

(A) Representative F2 seedling phenotypes resulting from a self cross of 06-932-30.

(B) Sibling plants from an outcross of *T pl-R30/T Pl-Rh* to *pl1-987/pl1-987*; *B1-Strong/B1-Strong*. A *pl1-B73/pl1-987*; *b1/B1-Strong* individual is shown as a comparison.

(C) Representative anthers of indicated genotypes showing *pl1-R30* is weakly expressed.

with the increased aleurone pigmentation observed in advanced filial generations of 1:1 segregating *rpd1-1* families (Figure 2). We determined the 5′-methylcytosine (5meC) profiles at the 5′ border of the *Pl1-Rhoades doppia* fragment (see Supplemental Figure 7A online) by sequencing PCR amplicons from bisulfite-treated genomic DNA isolated from individual aleurones. We compared 5meC profiles of DNA isolated from darkly pigmented (molecularly genotyped as *rpd1-1/rpd1-1*) and lightly pigmented (molecularly genotyped as *+/rpd1-1*) kernels representing the F7 and F9 generations and in unconditioned control (+/+) kernels (see Supplemental Figure 7B online). These profiles indicate that cytosines both 5′ of and within the *doppia* fragment are relatively hypomethylated (see Methods) in both F7 (10/37 hypomethylated cytosines) and F9 (14/37 hypomethylated cytosines) darkly pigmented kernels compared with their respective lightly pigmented siblings profiles (see Supplemental Figures 7C and 7D online). Specific cytosines in all contexts (CHG, CHH, and CG) were affected by the loss of RPD1 function, although predominant differences were biased for CHG and CHH context. These data confirm earlier results obtained with methylation-sensitive restriction enzymes (Hale et al., 2007) showing RPD1-dependent maintenance of 5meC patterns. In the presence of RPD1, 5meC patterns remained relatively unaffected in this region, even among the F7 and F9 genotypes (see Supplemental Figures 7C and 7D online). While aleurone pigmentation is correlated with the loss of RPD1 and 5meC across this region, the increased pigmentation seen in the presence of RPD1 following *trans*-generational conditioning is not. This result indicates that either 5meC patterns are differentially conditioned at regions not evaluated in our analysis or that a distinct epigenetic feature at this region is modified by such breeding designs.

Kernel Pigmentation Occurs in Other siRNA Biogenesis Mutants

Three other siRNA biogenesis pathway components are required for maintaining repressed *Pl′* states, including REQUIRED TO MAINTAIN REPRESSION1 (RMR1), a SUCROSE NONFERMENTING2-like ATPase (Hale et al., 2007); MEDIATOR OF PARAMUTATION1 (MOP1), a putative RNA-dependent RNA polymerase (Woodhouse et al., 2006; Alleman et al., 2006); and one of three presumed second largest subunits of Pol IV isoforms, RMR7/NRPD2a (Sidorenko et al., 2009; Stonaker et al., 2009). We found aleurone pigmentation in ear progenies segregating 1:1 for homozygous *rmr1*, *mop1*, and *rpd2a* mutants and heterozygous siblings. Cosegregation analyses, performed as described above for *rpd1*, indicated that RMR1, MOP1, and RPD2a also contribute to repression of *Pl1-Rhoades* in the aleurone layer (Figures 5A and 5B). However, distinctive from the loss of *rpd1*, we did not see evidence for enhancement of pigmentation in subsequent generations.

DISCUSSION

The characterization of meiotically heritable epialleles broadens our understanding of how selectable traits can be manipulated and transmitted across generations. Our results indicate that *trans*-generational Pol IV function defines specific expression domains of endogenous maize alleles. We find that epigenetic

Table 2. Cosegregation of Aleurone Pigmentation with *pl1-R30* Homozygotes

		No. of F2 Individuals Grown from Pigmented Kernels with Indicated Genotypes		
Genotype of Selfed F1 Parent	No. of Progeny Ears	*Pl1-Rhoades/Pl1-Rhoades*	*Pl1-Rhoades/pl1-R30*	*pl1-R30/pl1-R30*
Pl1-Rhoades/pl1-R30; *+/rpd1-1*	2	15	12	6

conditioning of *Pl1-Rhoades* across multiple generations in *rpd1* mutants converts a null allele for aleurone expression into a heritable, fully functional, dominant form. Our genetic analyses using *Pl1-Rhoades* derivatives and closely related alleles provide a correlation between nearby repetitive sequences and endogenous allele structures subject to siRNA-directed regulation. A similar relationship is supported by comparative genomics and siRNA signatures in divergent *Arabidopsis* accessions (Hollister et al., 2011).

Our results contrast with those of other known epialleles subject to siRNA-based control in that heritable changes in *Pl1-Rhoades* regulation are conditioned in the absence of Pol IV, which is required for RdDM (Haag and Pikaard, 2011). Both *Arabidopsis* silent epialleles *FWA* and *SDC* contain repetitive features targeted by RdDM, yet *FWA* is not derepressed in RdDM mutants (Cao and Jacobsen, 2002; Chan et al., 2006a) and the derepressed *SDC* found in similar mutants is not meiotically heritable (Chan et al., 2006b; Henderson and Jacobsen, 2008). These contrasts may reflect the general differences in haplotype structures (Hale et al., 2009) and/or Pol IV functions (Stonaker et al., 2009) seen in grasses relative to eudicots.

It remains unknown whether restriction of *Pl1-Rhoades* expression in the presence of siRNAs is mechanistically related to paramutation interactions occurring between *Pl1-Rhoades* states. The 3′ sequences required for paramutation interactions are not necessary for aleurone expression, but the 5′ *doppia* fragment may be necessary for paramutations. This hypothesis predicts that a genetic difference, defined by 3′ regulatory sequences, distinguishes the *Pl1-Rhoades* and *Pl1-Blotched* haplotypes, which is consistent with linkage data indicating that the Blotched factor is located ~1 centimorgan (cM) distal of *Pl1-Rhoades* (Rhoades, 1948). The recovery of *pl1-R30* from a screen for recombinant alleles between *pl1-B73* and *Pl1-Rhoades* demonstrates that the paramutagenic elements of *Pl1-Rhoades* are tightly linked but separable, from the *Pl1-Rhoades* coding sequence. The screen recovered one recombinant haplotype among ~13,655 chromatids screened, placing the paramutagenic element(s) ~0.0073 cM distal of the *Pl1-Rhoades* coding sequence. However, this estimate assumes that all such recombinants were recognized in our phenotypic screen.

Molecular, genetic, and phenotypic analyses of *pl1-R30* indicate it is different from its progenitor alleles. *pl1-R30* is weakly expressed in seedlings, unlike both *Pl1-Rhoades* and *pl1-B73*, and weakly expressed in anthers like *pl1-B73* but unlike *Pl1-Rhoades*. The *pl1-B73* enhancer for seedling expression may be 5′ of the coding sequence, and the *pl1-B73* enhancer for anther expression may be 3′ of the coding sequence. However, in *Pl1-Rhoades*, both tissue-specific enhancers, or a single enhancer functioning in both seedlings sheaths and anthers, could be 3′ of the coding sequence. The paramutagenic element(s) of *Pl1-Rhoades* is located 3′ of the coding sequence, which could be identical to or closely linked to an enhancer(s) required for high expression. This scenario is similar to the model of the maize *B1-Intense* (*B1-I*) haplotype, in which an enhancer-type element ~100 kb 5′ of the *B1-I* coding region regulates both high expression and paramutagenic activity (Stam et al., 2002a, 2002b). Although the *cis*-acting features

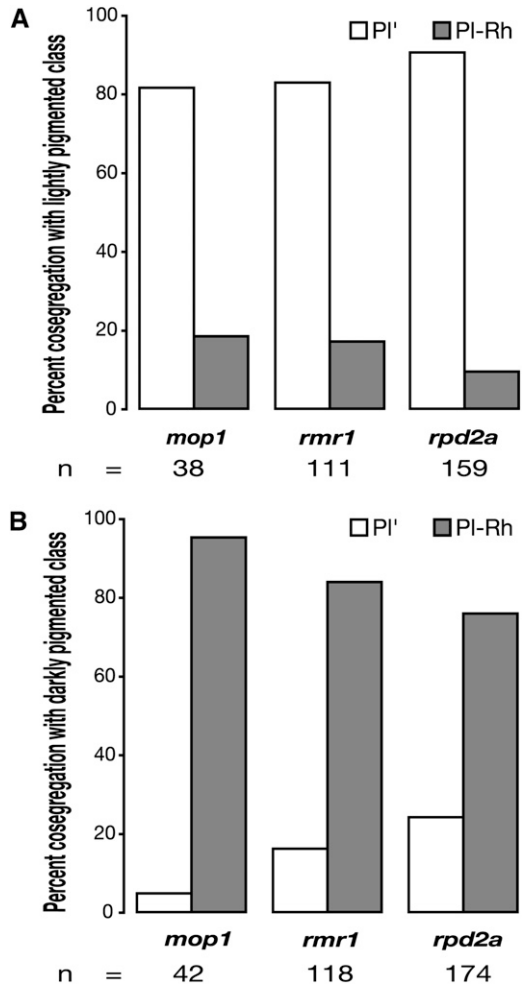

Figure 5. Aleurone Pigmentation in siRNA Biogenesis Mutants.

(A) Histogram showing the percentage of mature plant phenotypes (Pl′ and Pl-Rh as described in Figure 1) among progeny segregating 1:1 for heterozygotes and homozygous mutants for each of the siRNA biogenesis factors listed, after selection of kernels with the lightest pigmentation of the progeny.

(B) Same analyses as in **(A)** after selection of kernels with the darkest pigmentation.

required for *Pl1-Rhoades* paramutation interactions have not been identified, genetic and molecular evidence suggests that regulatory regions of *pl1* and/or RNA transcripts produced by the *pl1* coding sequence could be important for these *trans*-homolog interactions (Gross and Hollick, 2007). Thus, the *trans*-sensing interactions between *pl1* haplotypes may occur between distal *cis*-regulatory sequences.

It will be important to determine the requirement of the 5′ *doppia* fragment for both paramutation interactions between *Pl1-Rhoades* alleles and its aleurone expression capacity. Cytosine methylation patterns at this feature appear identical in both *Pl′* and *Pl-Rh* states (Hale et al., 2007). Most of the RdDM-like factors identified to date in forward genetic screens for paramutation defects may primarily affect the transcriptional status of *Pl1-Rhoades* via their action on the attendant *doppia* fragment, and these effects may be unrelated to the paramutation process responsible for *trans*-homolog communication. siRNAs alone appear to be insufficient for certain aspects of paramutation interactions between *Pl1-Rhoades* alleles (Erhard and Hollick, 2011; Barbour et al., 2012). For example, the 64% of siRNAs dependent on RMR1 function (Hale et al., 2009) are not required for the acquisition of *Pl′* states (Hale et al., 2007), and the 85% of siRNAs dependent on RMR7/NRPD2a are not required to maintain the meiotically heritable *Pl′* state (Stonaker et al., 2009). Therefore, the presumed RdDM-like mechanism suppressing *Pl1-Rhoades* expression in the aleurone may be functionally distinct from that which facilitates the *trans*-homolog interactions between *Pl1-Rhoades* alleles.

Our findings implicate the 5′ *doppia* fragment as a component of the regulatory module that conditions strong aleurone expression after transmission from siRNA mutants. A similar 226-bp *doppia* fragment acts as an aleurone-specific promoter in the *R-r* haplotype of the *red1* (*r1*) locus (Walker et al., 1995), which encodes an anthocyanin regulator unrelated to *pl1*, suggesting that the *doppia* fragment in the promoter regions of the four *pl1* alleles we examined (Figure 3C) may be responsible for their aleurone expression. It remains possible that heritable loss of Pol IV–directed cytosine methylation patterns within and surrounding the *doppia* sequence 5′ of *Pl1-Rhoades* influences or facilitates the *trans*-generational increase in pigmentation observed after multiple generations of conditioning in an *rpd1* mutant background. It is also possible that other epigenetic regulatory features are progressively altered by such treatments.

In contrast with the progressive and meiotically heritable enhancement of aleurone pigmentation reported here, other developmental defects typically seen in *rpd1* mutant plants such as problems with leaf polarity are not heritable (Parkinson et al., 2007). The difference in heritability of *rpd1* mutant phenotypes in the mature plant and the *Pl1-Rhoades* aleurone expression domain may reflect a fundamental difference in the function of RdDM in embryo- and endosperm-derived cells. This difference may also reflect functional diversity in the allele or haplotype structures of RPD1 targets, as seen between *Pl1-Rhoades* and its derivatives. It also remains unclear why *doppia*-associated *pl1* alleles conditioned in the absence of other siRNA biogenesis components are not progressively enhanced in pigmenting potential. This observation implicates a role of Pol IV in defining meiotically heritable regulatory patterns unrelated to a presumed RdDM pathway.

Pol IV function represents a molecular link between developmental gene control in maize and TE-associated epiallele regulation. Alleles, or haplotypes, that undergo paramutation are seemingly exceptional, but TE-associated haplotypes affected by Pol IV action may be far more numerous. We speculate that Pol IV has been co-opted during maize evolution and germplasm improvements to define the expression pattern of specific alleles that have incorporated repeat-like features. Changes to the heterochromatic component, as defined by maize Pol IV, thus leads to the appearance of phenotypic variation as previously surmised (McClintock, 1951). Our results indicate that Pol IV, together with repetitive genomic features, constitute a nuclear system serving as a capacitor of cryptic, heritable epigenetic variation available for breeding and evolution.

METHODS

Nomenclature

Alleles, phenotypes, and genotypes of maize (*Zea mays*) are designated as described (Hollick et al., 2005). The "|" delineates *cis*-elements in recombinant haplotypes, where descriptors on the left of the "|" indicate centromere proximal elements, and descriptors on the right of the "|" describe centromere distal features. For SSLP markers, polymorphisms derived from the *T Pl1-Rhoades*/*T Pl1-Rhoades* parent (see below) are referred to as "Rhoades" types, and polymorphisms derived from the B73 inbred line parent are referred to as "B73" types. Female-derived factors are placed before male-derived factors when stating diploid genotypes. Anther pigmentation is visually assessed using a 1 to 7 graded ACS as previously described (Hollick et al., 1995).

Genetic Stocks

The *rpd1-1* and *rpd1-2* stocks used to generate families segregating 1:1 for *rpd1-1* and *rpd1-2* homozygotes and heterozygous siblings (Figures 1 and 2, respectively) were previously described (Hollick et al., 2005; Parkinson et al., 2007) and contain the plant color genotypes *Pl1-Rhoades* (*Pl′*); *b1*; *c1*; *R-r*.

For the *Pl1-Rhoades* recombinant screen, the B73 inbred line and a *Pl1-Rhoades* line homozygous for the *T6-9 (043-1)* interchange (*T*), *T Pl1-Rhoades*/*T Pl1-Rhoades* (*T Pl′*/*T Pl′*), are as described (Hollick et al., 2005; Gross and Hollick, 2007). The *9S* portion of the *T Pl1-Rhoades* chromosome carries a recessive *waxy1* (*wx1*) allele and, thus, selection of opaque waxy kernels among starchy kernels aides selection of *T Pl1-Rhoades* homozygotes. The translocation breakpoint 1.5 cM from *Pl1-Rhoades* (±1.1 cM) represents a dominant semisterility locus (Hollick et al., 2005). Translocation heterozygotes produce ~50% sterile pollen, yet translocation homozygotes produce ~100% fertile pollen (Patterson, 1994). *T Pl-Rh*/*T Pl-Rh* stocks were obtained by capturing a revertant *Pl-Rh* state from an ACS 7, *rpd1-1*/*rpd1-1*; *T Pl′*/*T Pl′* individual as described (Hollick et al., 2005). Additional *Pl-Rh*/*Pl-Rh* testers are as described (Hollick et al., 2005; Gross and Hollick, 2007). A null *pl1* stock, (*pl1-987*/*pl1-987*; *B1-Strong*/*B1-Strong*) was provided by Karen Cone, University of Missouri, Columbia, MO. To generate screening material for recombinants between *pl1-B73* and *Pl1-Rhoades*, *pl1-B73*/*pl1-B73* females were crossed by *T Pl′*/*T Pl′* males. F1 (*pl1-B73*/*T Pl′*) individuals were crossed by *T Pl-Rh*/*T Pl-Rh* (ACS 7) males, and kernels resulting from this cross were screened as described below.

Inbred line CML52 used for the paramutation test (see Supplemental Table 4 online) was obtained from the North Central Regional Plant Introduction Stations, Ames, IA. Complementation tests indicate that the CML52 inbred line contains both a null *c1* allele and a null seed

component of the *r1* haplotype (*r-r*). Female and male parents, ear progenies examined, and kernel phenotypes are as follows: CML52, A632 (*c1*; *R-r*), 2, all colorless aleurones; CML52, K55 (*C1*; *r-r*), 2, all colorless aleurones; K55 (*C1*; *r-r*), CML52, 2, all colorless aleurones.

Color-converted A632 [*Pl1-Rhoades* (*Pl′*); *b1*; *c1*; *R-r*] stocks used for outcrosses are described by Hollick et al. (2005). Color-converted Mo17 stocks [>93% Mo17; *Pl1-Rhoades* (*Pl′*); *B1-Mo17*; *c1*; *R-r*] used for outcrosses were established through recurrent backcrosses to the inbred line in the same manner as described by Hollick et al. (2005). The A619 [*Pl1-Rhoades* (*Pl-Rh*); *b1*; *c1*; *R-r*] stock used as a control for bisulfite conversion (see below) was derived by introgressing *T Pl-Rh* containing a null *c1* allele into the color-converted A619 [*Pl1-Rhoades* (*Pl-Rh*); *b1*; *C1*; *R-r*] stock described by Hollick et al. (2005).

Plant 06-932-30 (*T pl1-R30*/*T Pl-Rh*) was selfed, and resulting progeny were genotyped for the *umc2006* marker to identify *pl1-R30* homozygotes. Plant 06-932-30 was also crossed to both *pl1-CO159*/*pl1-CO159* and *pl1-987*/*pl1-987*; *B1-Strong*/*B1-Strong* recessive testers. Individuals from segregating families were genotyped for the *umc2006* polymorphism to follow the specific *pl1* haplotypes (see Supplemental Table 6 online).

Screening for *Pl1-Rhoades* Recombinant *pl1-R30*

The *T6-9 (043-1)* (*T Pl1-Rhoades*) interchange chromosomes, *T Pl′* and *T Pl-Rh*, provide genetic markers linked to *Pl1-Rhoades* that facilitate the detection of recombination events in specific intervals (I, II, and III) along the *T Pl1-Rhoades* chromosome (see Supplemental Figure 4A online). To provide F1 materials required for the desired recombination event, *pl1-B73*/*pl1-B73* was crossed by *T Pl′*/*T Pl′* (see Supplemental Figure 4B online). Recombination events occurring between B73 chromosomes and specific intervals of the *T Pl′* chromosome were detected following a testcross by a *T Pl-Rh*/*T Pl-Rh* tester (see Supplemental Figure 4B and Supplemental Table 5 online). Waxy-type kernels, most containing embryos homozygous for *T6-9* chromosomes, were selected and planted. Because *Pl1-Rhoades* resides only ~5.3 cM from the *wx1* mutation, ~95% of the seedlings grown from waxy seeds will contain parental-type chromosomes with no recombination events between *wx1* and *Pl1-Rhoades*. Recombination within interval I, the 3.9 cM between the *wx1* mutation and the *T6-9* breakpoint, unlinks the two markers by placing the *wx1* mutation on a structurally normal chromosome *9*, resulting in nonrecombinant + *pl1-B73* chromosomes being selected through pseudolinkage to *wx1* in balanced gametes (see Supplemental Table 5 online). Recombination in intervals II and III near the *pl1* locus may disrupt *cis*-linkage of paramutagenic elements and *Pl1-Rhoades* (see Supplemental Figure 4A and Supplemental Table 5 online). Paramutagenic elements may be either centromere-proximal of the *Pl1-Rhoades* coding sequence (see Supplemental Table 5 online, scenario A) or distal (see Supplemental Table 5 online, scenario B). These possible scenarios can be distinguished by generating recombinant *pl1* haplotypes that either gain or lose paramutagenic elements. If paramutagenic elements are proximal of the *Pl1-Rhoades* coding sequence (scenario A), a recombinant haplotype with paramutagenic elements and the *pl1-B73* coding sequence could be generated. Alternatively, if paramutagenic elements reside distal of the *Pl1-Rhoades* coding sequence (scenario B), a nonparamutagenic *Pl1-Rhoades* haplotype can be recovered.

Waxy (*wx*/*wx*/*wx*) kernels (n = 13,655) resulting from *pl1-B73*/*wx T Pl′* × *wx T Pl-Rh*/*wx T Pl-Rh* were planted in vermiculite and sand and grown without fertilizer to maximize anthocyanin pigmentation. Approximately 2-week-old seedlings were examined for anthocyanin pigmentation in the first seedling sheath. Only the most intensely pigmented seedlings resembling Pl-Rh phenotypes were selected (n = 360), and an unrecorded number of seedlings with relatively less pigmentation were discarded. Rescued plants were transplanted into the field and grown to maturity. Given the ~3.8-cM distance between the *wx1* and *pl1* loci, ~518 darkly pigmented *T pl1-B73*/*Pl-Rh* seedlings were expected. As *pl1-B73* confers intense pigmentation to seedling sheaths much like *Pl-Rh*, the rescued plants were genotyped to select *Pl1-Rhoades*/*Pl1-Rhoades* plants. DNA was extracted from Pl-Rh–type seedlings as described below and SSLP genotyped for the *pl1* coding sequence using *phi031* SSLP primers (Lawrence et al., 2007) as described (Gross and Hollick, 2007): 5′-GCAACAGGTTACATGAGCTGACGA-3′ and 5′-CCAGCGTGCTGTTCCAGTAGTT-3′. Plants with *pl1-B73*/*Pl1-Rhoades* *phi031* polymorphisms were discarded (354 of 360 were *pl1-B73*/*Pl1-Rhoades*). The six remaining *Pl1-Rhoades*/*Pl1-Rhoades* individuals were scored for their ACS and pollen phenotypes as described (Hollick et al., 2005). Of the remaining 6 *Pl1-Rhoades*/*Pl1-Rhoades* plants, all were fully fertile (*T*/*T*), but five had Pl′-like phenotypes and were discarded. Only one *Pl1-Rhoades*/*Pl1-Rhoades* individual (06-932-30) had fully fertile pollen and ACS 7 anthers. Select *Pl1-Rhoades*/*Pl1-Rhoades* individuals from family 06-932 were genotyped for the *bnlg2249* SSLP polymorphism (Lee et al., 2002) to confirm the presence of a recombination event distal to the *pl1* locus using the primer pairs 5′-AGGATCCCCTAGCAAAAGGA-3′ and 5′-CCCCCTAGTTCGTTGCATAA-3′.

Mapping of Recombinant *pl1-R30*

All SSLP mapping was performed using DNA from the individual heterozygous for the recombinant *pl1* allele, 06-932-30 (*T pl-R30*/*T Pl1-Rhoades*). The maize FPC map (http://www.gramene.org and http://www.maizesequence.org) was used to find sequenced or partially sequenced BACs anchored to maize FPC BAC contig 280, on which *pl1-B73* had been placed. Genetic distances between *pl1*, *umc2006* (Lee et al., 2002; 5′-AGTCCATCACCATCCCTGGC-3′ and 5′- GCAGAACTATTGTCAGTTAACCTTGCAT-3′), and *bnlg2249* markers were calculated using the maize IBM2 2004 Neighbors 6 map available at MaizeGDB (http://www.maizegdb.org; Lee et al., 2002). To coordinate the genetic distance between this high-resolution genetic map and F2 data, genetic distances of the IBM2 2004 Neighbors map were divided by a factor of 3.8 (Yao et al., 2002). This method places *pl1* ~4.71 cM centromere proximal of *umc2006* and 17.5 cM proximal of *bnlg2249*.

Molecular Analyses

For *Pl1-Rhoades* expression analysis (Figure 1B), aleurone layers were hand-dissected from individual developing kernels 25 d after pollination of an ear from a Pl′-like (+/*rpd1-1*) plant by pollen from a Pl-Rh–like (*rpd1-1*/*rpd1-1*) plant, and RNA was isolated using TRIzol reagent (Invitrogen) following the manufacturer's protocol. cDNA was generated as previously described (Hale et al., 2007) using 1 μg of total RNA as template. Separate reactions were performed with RNA from four independent biological replicates for each of the two pigment/genotypes using no reverse transcriptase to control for genomic DNA contamination. Resulting cDNA samples were PCR amplified for 27 cycles using *Pl1-Rhoades*–specific primers (Gross and Hollick, 2007) and primers specific to *Ala aminotransferase* as described (Hale et al., 2007), yielding a 171-bp product and a 290-bp product, respectively. RT-PCR products were sized on a 2% agarose gel and stained with ethidium bromide for visualization and qualitative comparison between samples.

For sequencing of *c1* and *pl1* alleles, genomic DNA was isolated from seedling or mature plant leaves as described (Hale et al., 2007). DNA from Pl′-type plants in a 1:1 *rpd1*-segregating family from stocks described above was amplified via PCR using *c1*-specific primers homologous to sequences in the 5′ untranslated region and intron 2, respectively: 5′- CGTAGTTAGCGCCACTGCTA-3′ and 5′-GAACAGATGAATTCGCAGCA-3′. DNA from CML52 inbred plants was PCR amplified using *pl1*-specific primers homologous to sequences 5′ of the *doppia* fragment and the intron 1–exon 2 boundary, respectively: 5′-TGTTTTGTCTTGACTGAGGGAGAAG-3′ and 5′-AAACCTGCACACACACCATC-3′. PCR amplicons were purified as described (Hale et al., 2007) and sequenced at the UC Berkeley DNA Sequencing Facility (http://mcb.berkeley.edu/barker/dnaseq/index.html).

Derived cleaved amplified polymorphic sequence primers (Neff et al., 1998) were designed to molecularly identify the *rpd1-1* lesion (Erhard et al., 2009): 5′-TAGAAGTTCTTATGGGCAGCCAATAGGG-3′ and 5′-GGGTGTTCCAAAGCTCCATA-3′. During the PCR, the forward primer introduces a *Bgl*I restriction site only when amplifying genomic DNA or cDNA containing the wild-type sequence over the region containing the *rpd1-1* lesion. PCR amplicons (139 bp) were digested for 1 h at 37°C with *Bgl*I (New England Biolabs) and analyzed by agarose gel electrophoresis to determine the restriction polymorphism (22 bp) of each sample.

All materials for *pl1-R30* transcript analyses were grown in soil and vermiculite with fertilizer under standard greenhouse conditions. Sheath tissue below the 1st leaf was collected from 2-week-old seedlings. Developing tassel florets were collected just prior to opening, identified by their proximity to florets that had previously opened and extruded anthers. All tissues for transcript analysis were collected near mid-day. RNA was extracted and RT-PCR was performed as described (Gross and Hollick, 2007) starting with 10 μg total RNA.

A probe for the −1300 region of *Pl1-Rhoades* used in DNA gel blot analyses (see Supplemental Figure 5 online) was generated as follows. Available *Pl1-Rhoades* sequence was compared with additional maize sequences deposited in GenBank using BLASTn (Altschul et al., 1997). A region extending from −1318 through −2316 was found to be unique to *pl1*. This sequence was amplified by PCR using primers Bh_Eco_L (5′-TGGCCC TTCAATCCAGTGGTA-3′) and Bh_Eco_R (5′-CCCCCACTT-TGTTCACTTTG-3′) from the *Pl1-Blotched* 2.4-kb *Eco*RI plasmid provided by Karen Cone, University of Missouri, Columbia, MO. PCR conditions were as follows: 95°C for 35 s, 60°C for 35 s, 72°C for 1 min, for 35 cycles. PCR amplicons for the −1300 probes were gel purified using the Freeze 'N Squeeze gel extraction kit (Bio-Rad) prior to radiolabeling. DNA for DNA gel blot analysis was extracted as described (Voelker et al., 1997). Four micrograms of genomic DNA was cut with indicated enzyme according to the manufacturer's instructions (New England Biolabs), separated on 1% agarose gels, and blotted to Hybond-N membranes (GE Healthcare Life Sciences). The −1300 probe was labeled as described (Feinberg and Vogelstein, 1983). Hybridized blots were exposed to phosphor screens for 3 d and imaged as described (Gross and Hollick, 2007).

Bisulfite Sequencing

Darkly blotched and lightly blotched aleurones were hand-dissected from kernels of F7 and F9 progeny ears and from kernels of *Pl1-Rhoades* (A619) 2 d postimbibition, and genomic DNA was isolated as previously described (Voelker et al., 1997) with the following modifications: Aleurones were frozen in liquid nitrogen and vigorously ground using a mortar and pestle with lysis buffer (7 M urea, 0.25 M NaCl, 50 mM Tris-HCl, pH 8.0, 1% *N*-laurylsarcosine, 20 mM EDTA, and 0.25% β-mercaptoethanol) until thawed. After a 5-min incubation at 37°C, DNA samples were extracted from pulverized aleurone tissue with phenol/chloroform/isoamyl alcohol, precipitated in isopropanol, and resuspended in TE. Five hundred nanograms of genomic DNA was bisulfite converted following manufacturer's specifications using the EZ DNA Methylation Kit (Zymo Research). Degenerate primers (Doppia-bis-F, 5′-GTGATTAGGTAGAAGTGGGAG-3′, and Doppia-bis-R: 5′-TAC-CRACRAAAATCACCTATTTTC-3′) were designed using the Kismeth web suite (Gruntman et al., 2008) to amplify the 5′ portion of the *doppia* fragment (−660 to −190 nucleotides from the *Pl1-Rhoades* transcription start site) from both untreated and bisulfite-treated templates. Gel-purified (Freeze 'N Squeeze gel extraction kit) 470-bp PCR amplicons were cloned using the pGEM-T Easy vector system (Promega) following vendor instructions, and the resulting plasmids were transformed into TOP10 cells (Invitrogen). Validated clones were sequenced by the Plant-Microbe Genomics Facility (The Ohio State University, Columbus, OH) using the Doppia-bis-F primer. Geneious software (Biomatters) was used to trim sequences and perform quality control before bisulfite analysis with Kismeth. Data included in bisulfite sequence analysis using the Kismeth web suite (parameters: 0.8 min fraction of positive matches; 0.25 min fraction of length) comprise sequenced clones from one A619 aleurone, two F7 light blotchy aleurones, three F7 dark blotchy aleurones, three F9 light blotchy aleurones, and three F9 dark blotchy aleurones. Standard error and analysis of variance tests were performed with JMP software (SAS). We called a cytosine relatively hypomethylated if the percentage of methylation averaged from the biological replicates of one genotype was lower by at least one standard error than the average of the comparable cytosine from another genotype.

Accession Numbers

DNA sequence data from this article can be found in the GenBank/EMBL database under the following accession numbers: *c1-Hbr* (JX556412) and *Pl1-CML52* (JX556413)

Supplemental Data

The following materials are available in the online version of this article.

Supplemental Figure 1. *c1-Hbr* Allele Structure.

Supplemental Figure 2. Representative Aleurone Pigmentation Phenotypes.

Supplemental Figure 3. Aleurone Pigmentation in Stocks Containing *Pl1-CML52*.

Supplemental Figure 4. Selection of *pl1-R30*.

Supplemental Figure 5. DNA Gel Blot Analysis of *pl1-R30*.

Supplemental Figure 6. RT-PCR Analysis of *pl1-R30.*

Supplemental Figure 7. Cytosine Methylation at the *Pl1-Rhoades doppia* Element.

Supplemental Table 1. *c1-n* Cosegregation with Aleurone Pigment Phenotype.

Supplemental Table 2. Aleurone Pigmentation Phenotypes of Ear Progeny Resulting from Outcrossing Individuals Grown from Pigmented Kernels.

Supplemental Table 3. *Pl1-CML52* Cosegregation with Aleurone Pigment Phenotype.

Supplemental Table 4. Progeny Phenotypes Resulting from Cross of *Pl1-CML52/T Pl′* × *T Pl-Rh/T Pl-Rh*.

Supplemental Table 5. Frequencies and Descriptions of Expected Genotypes and Phenotypes of *wx1/wx1* Seedlings and Plants Resulting from *pl1-B73/T Pl′* × *T Pl-Rh/T Pl-Rh*.

Supplemental Table 6. Anther Phenotypes of Genotyped Progeny Resulting from Outcrosses of 06-932-30 (*T pl1-R30/T Pl-Rh*) to Indicated Testers.

Supplemental Table 7. Anther Phenotypes of Progeny Resulting from Outcrosses of 06-932-30 (*T pl1-R30/T Pl-Rh*) to Indicated Testers.

Supplemental Table 8. Anther and Seedling Phenotypes and *umc2006* Genotypes for F2 Progeny of 06-932-30 (*T pl-R30/T Pl-Rh*).

Supplemental Table 9. *pl1-R30* and *Pl1-Blotched* Anther Phenotypes in *rpd1* Mutants.

ACKNOWLEDGMENTS

We thank Sheila McCormick and Karen Cone for helpful comments on the article. This work was supported by the National Research Initiative of the USDA Cooperative State Research, Education, and Extension Service (99-35301-7753, 2001-35301-10641, and 2006-35304-17399) and the National

Science Foundation (MCB-0419909). The views expressed are solely those of the authors and are not endorsed by the sponsors of this work.

AUTHOR CONTRIBUTIONS

K.F.E., S.E.P., S.M.G., J.R.B., and J.B.H. designed research. K.F.E., S.E.P., S.M.G., J.P.L., J.R.B., and J.B.H. performed research. K.F.E., S.E.P., S.M.G., J.P.L., J.R.B., and J.B.H. analyzed data. K.F.E. and J.B.H. wrote the article. K.F.E., S.E.P., S.M.G., J.P.L., J.R.B., and J.B.H. revised and edited the article and figures.

Received November 21, 2012; revised February 20, 2013; accepted February 26, 2013; published March 19, 2013.

REFERENCES

Alleman, M., Sidorenko, L., McGinnis, K., Seshadri, V., Dorweiler, J.E., White, J., Sikkink, K., and Chandler, V.L. (2006). An RNA-dependent RNA polymerase is required for paramutation in maize. Nature **442:** 295–298.

Altschul, S.F., Madden, T.L., Schäffer, A.A., Zhang, J., Zhang, Z., Miller, W., and Lipman, D.J. (1997). Gapped BLAST and PSI-BLAST: A new generation of protein database search programs. Nucleic Acids Res. **25:** 3389–3402.

Barbour, J.E., Liao, I.T., Stonaker, J.L., Lim, J.P., Lee, C.C., Parkinson, S.E., Kermicle, J., Simon, S.A., Meyers, B.C., Williams-Carrier, R., Barkan, A., and Hollick, J.B. (2012). required to maintain repression2 is a novel protein that facilitates locus-specific paramutation in maize. Plant Cell **24:** 1761–1775.

Cao, X., and Jacobsen, S.E. (2002). Role of the *Arabidopsis DRM* methyltransferases in de novo DNA methylation and gene silencing. Curr. Biol. **12:** 1138–1144.

Chan, S.W., Henderson, I.R., Zhang, X., Shah, G., Chien, J.S., and Jacobsen, S.E. (2006b). RNAi, DRD1, and histone methylation actively target developmentally important non-CG DNA methylation in *Arabidopsis*. PLoS Genet. **2:** e83.

Chan, S.W., Zhang, X., Bernatavichute, Y.V., and Jacobsen, S.E. (2006a). Two-step recruitment of RNA-directed DNA methylation to tandem repeats. PLoS Biol. **4:** e363.

Cocciolone, S.M., and Cone, K.C. (1993). *Pl-Bh*, an anthocyanin regulatory gene of maize that leads to variegated pigmentation. Genetics **135:** 575–588.

Cone, K.C., Cocciolone, S.M., Burr, F.A., and Burr, B. (1993a). Maize anthocyanin regulatory gene *pl* is a duplicate of *c1* that functions in the plant. Plant Cell **5:** 1795–1805.

Cone, K.C., Cocciolone, S.M., Moehlenkamp, C.A., Weber, T., Drummond, B.J., Tagliani, L.A., Bowen, B.A., and Perrot, G.H. (1993b). Role of the regulatory gene *pl* in the photocontrol of maize anthocyanin pigmentation. Plant Cell **5:** 1807–1816.

Erhard, K.F., Jr., and Hollick, J.B. (2011). Paramutation: A process for acquiring *trans*-generational regulatory states. Curr. Opin. Plant Biol. **14:** 210–216.

Erhard, K.F., Jr., Stonaker, J.L., Parkinson, S.E., Lim, J.P., Hale, C. J., and Hollick, J.B. (2009). RNA polymerase IV functions in paramutation in *Zea mays*. Science **323:** 1201–1205.

Feinberg, A.P., and Vogelstein, B. (1983). A technique for radiolabeling DNA restriction endonuclease fragments to high specific activity. Anal. Biochem. **132:** 6–13.

Gross, S.M., and Hollick, J.B. (2007). Multiple *trans*-sensing interactions affect meiotically heritable epigenetic states at the maize *pl1* locus. Genetics **176:** 829–839.

Gruntman, E., Qi, Y., Slotkin, R.K., Roeder, T., Martienssen, R.A., and Sachidanandam, R. (2008). Kismeth: Analyzer of plant methylation states through bisulfite sequencing. BMC Bioinformatics **9:** 371.

Haag, J.R., and Pikaard, C.S. (2011). Multisubunit RNA polymerases IV and V: Purveyors of non-coding RNA for plant gene silencing. Nat. Rev. Mol. Cell Biol. **12:** 483–492.

Hale, C.J., Erhard, K.F., Jr., Lisch, D., and Hollick, J.B. (2009). Production and processing of siRNA precursor transcripts from the highly repetitive maize genome. PLoS Genet. **5:** e1000598.

Hale, C.J., Stonaker, J.L., Gross, S.M., and Hollick, J.B. (2007). A novel Snf2 protein maintains *trans*-generational regulatory states established by paramutation in *Zea mays*. PLoS Biol. **5:** e275.

Henderson, I.R., and Jacobsen, S.E. (2008). Tandem repeats upstream of the *Arabidopsis* endogene *SDC* recruit non-CG DNA methylation and initiate siRNA spreading. Genes Dev. **22:** 1597–1606.

Hoekenga, O.A., Muszynski, M.G., and Cone, K.C. (2000). Developmental patterns of chromatin structure and DNA methylation responsible for epigenetic expression of a maize regulatory gene. Genetics **155:** 1889–1902.

Hollick, J.B., Kermicle, J.L., and Parkinson, S.E. (2005). *Rmr6* maintains meiotic inheritance of paramutant states in *Zea mays*. Genetics **171:** 725–740.

Hollick, J.B., Patterson, G.I., Asmundsson, I.M., and Chandler, V.L. (2000). Paramutation alters regulatory control of the maize *pl* locus. Genetics **154:** 1827–1838.

Hollick, J.B., Patterson, G.I., Coe, E.H., Jr., Cone, K.C., and Chandler, V.L. (1995). Allelic interactions heritably alter the activity of a metastable maize *pl* allele. Genetics **141:** 709–719.

Hollister, J.D., Smith, L.M., Guo, Y.L., Ott, F., Weigel, D., and Gaut, B.S. (2011). Transposable elements and small RNAs contribute to gene expression divergence between *Arabidopsis thaliana* and *Arabidopsis lyrata*. Proc. Natl. Acad. Sci. USA **108:** 2322–2327.

Jablonka, E., and Raz, G. (2009). Transgenerational epigenetic inheritance: Prevalence, mechanisms, and implications for the study of heredity and evolution. Q. Rev. Biol. **84:** 131–176.

Kasschau, K.D., Fahlgren, N., Chapman, E.J., Sullivan, C.M., Cumbie, J.S., Givan, S.A., and Carrington, J.C. (2007). Genome-wide profiling and analysis of *Arabidopsis* siRNAs. PLoS Biol. **5:** e57.

Lawrence, C.J., Schaeffer, M.L., Seigfried, T.E., Campbell, D.A., and Harper, L.C. (2007). MaizeGDB's new data types, resources and activities. Nucleic Acids Res. **35** (Database issue)**:** D895–D900.

Lee, M., Sharopova, N., Beavis, W.D., Grant, D., Katt, M., Blair, D., and Hallauer, A. (2002). Expanding the genetic map of maize with the intermated B73 x Mo17 (IBM) population. Plant Mol. Biol. **48:** 453–461.

McClintock, B. (1951). Chromosome organization and genic expression. Cold Spring Harb. Symp. Quant. Biol. **16:** 13–47.

Neff, M.M., Neff, J.D., Chory, J., and Pepper, A.E. (1998). dCAPS, a simple technique for the genetic analysis of single nucleotide polymorphisms: Experimental applications in *Arabidopsis thaliana* genetics. Plant J. **14:** 387–392.

Nobuta, K., et al. (2008). Distinct size distribution of endogeneous siRNAs in maize: Evidence from deep sequencing in the mop1-1 mutant. Proc. Natl. Acad. Sci. USA **105:** 14958–14963.

Parkinson, S.E., Gross, S.M., and Hollick, J.B. (2007). Maize sex determination and abaxial leaf fates are canalized by a factor that maintains repressed epigenetic states. Dev. Biol. **308:** 462–473.

Patterson, E.B. (1994). Translocations as genetic markers. In The Maize Handbook, M. Freeling and V. Walbot, eds (New York: Springer-Verlag), pp. 361–363.

Rhoades, M.M. (1948). Interaction of *Bh* with recessive *c*. Maize Newsletter **22:** 9.

Richards, E.J. (2011). Natural epigenetic variation in plant species: A view from the field. Curr. Opin. Plant Biol. **14:** 204–209.

Scheffler, B., Franken, P., Schütt, E., Schrell, A., Saedler, H., and Wienand, U. (1994). Molecular analysis of *C1* alleles in *Zea mays* defines regions involved in the expression of this regulatory gene. Mol. Gen. Genet. **242:** 40–48.

Schnable, P.S., et al. (2009). The B73 maize genome: Complexity, diversity, and dynamics. Science **326:** 1112–1115.

Sidorenko, L., Dorweiler, J.E., Cigan, A.M., Arteaga-Vazquez, M., Vyas, M., Kermicle, J., Jurcin, D., Brzeski, J., Cai, Y., and Chandler, V.L. (2009). A dominant mutation in *mediator of paramutation2*, one of three second-largest subunits of a plant-specific RNA polymerase, disrupts multiple siRNA silencing processes. PLoS Genet. **5:** e1000725.

Slotkin, R.K., and Martienssen, R. (2007). Transposable elements and the epigenetic regulation of the genome. Nat. Rev. Genet. **8:** 272–285.

Stam, M., Belele, C., Dorweiler, J.E., and Chandler, V.L. (2002a). Differential chromatin structure within a tandem array 100 kb upstream of the maize *b1* locus is associated with paramutation. Genes Dev. **16:** 1906–1918.

Stam, M., Belele, C., Ramakrishna, W., Dorweiler, J.E., Bennetzen, J.L., and Chandler, V.L. (2002b). The regulatory regions required for *B'* paramutation and expression are located far upstream of the maize *b1* transcribed sequences. Genetics **162:** 917–930.

Stonaker, J.L., Lim, J.P., and Erhard, K.F., Jr., and Hollick, J.B. (2009). Diversity of Pol IV function is defined by mutations at the maize *rmr7* locus. PLoS Genet. **5:** e1000706.

Studer, A., Zhao, Q., Ross-Ibarra, J., and Doebley, J. (2011). Identification of a functional transposon insertion in the maize domestication gene *tb1*. Nat. Genet. **43:** 1160–1163.

Voelker, R., Mendel-Hartvig, J., and Barkan, A. (1997). Transposon-disruption of a maize nuclear gene, *tha1*, encoding a chloroplast SecA homologue: In vivo role of cp-SecA in thylakoid protein targeting. Genetics **145:** 467–478.

Walker, E.L., Robbins, T.P., Bureau, T.E., Kermicle, J., and Dellaporta, S.L. (1995). Transposon-mediated chromosomal rearrangements and gene duplications in the formation of the maize *R-r* complex. EMBO J. **14:** 2350–2363.

Wang, Q., and Dooner, H.K. (2006). Remarkable variation in maize genome structure inferred from haplotype diversity at the *bz* locus. Proc. Natl. Acad. Sci. USA **103:** 17644–17649.

Woodhouse, M.R., Freeling, M., and Lisch, D. (2006). Initiation, establishment, and maintenance of heritable *MuDR* transposon silencing in maize are mediated by distinct factors. PLoS Biol. **4:** e339.

Yao, H., Zhou, Q., Li, J., Smith, H., Yandeau, M., Nikolau, B.J., and Schnable, P.S. (2002). Molecular characterization of meiotic recombination across the 140-kb multigenic *a1-sh2* interval of maize. Proc. Natl. Acad. Sci. USA **99:** 6157–6162.

Zhang, Q., Arbuckle, J., and Wessler, S.R. (2000). Recent, extensive, and preferential insertion of members of the miniature inverted-repeat transposable element family *Heartbreaker* into genic regions of maize. Proc. Natl. Acad. Sci. USA **97:** 1160–1165.